

## New Asymptotics for Old Wave Equations

JOHN R. KLAUDER

Wave equations govern the propagation of acoustical or optical fields in diverse physical settings of interest to oceanographers, geologists, atmospheric scientists, among others. For wavelengths much smaller than all other length scales in the system the wave equation solution is generally expressed as a superposition of waveforms, each of which is determined by properties of the rays of geometrical acoustics or optics. Typically such solutions are accurate except in the vicinity of one or another caustic surface such as those defined as a surface across which a jump in the number of rays tracing through each point occurs. When numerous caustic surfaces exist, which is the generic situation, standard asymptotic solutions prove unsuitable. In this report a new asymptotic expression that overcomes deficiencies in previous approximations is introduced and characterized in an elementary way.

WAVE EQUATIONS FOR A SINGLE-component field  $\phi$  of the general form

$$ik^{-1} \frac{\partial \phi(x, z)}{\partial z} = H(-ik^{-1} \frac{\partial}{\partial x}, x, z) \phi(x, z) \quad (1)$$

have a variety of applications. Here  $k$  denotes the nominal wave number,  $z$  a propagation distance,  $x$  a transverse coordinate, and  $H$  the (self-adjoint) generator of propagation. Such equations have applications in unidirectional acoustical and optical propagation problems (1). If  $z$  is replaced by  $t$ , the time, and  $k^{-1}$  replaced by  $\hbar/2\pi$ , where  $\hbar$  is Planck's constant, then Eq. 1 describes a general one-dimensional quantum mechanics problem. In any case it follows for all  $z$  that

$$\int |\phi(x, z)|^2 dx = \int |\phi(x, 0)|^2 dx \quad (2)$$

which should normally be finite, independent of the various physical interpretations for  $\phi$ .

One particular solution of Eq. 1 denoted by  $J(x, R; x', 0)$  is called the propagator and is characterized by the initial condition

$$\lim_{R \rightarrow 0} J(x, R; x', 0) = \delta(x - x') \quad (3)$$

The propagator represents the response at position  $x$  and distance  $R$  to a normalized point source at position  $x'$  and distance 0. For many problems  $J$  itself is the field of physical interest, and in our discussion we shall also assume this is the case.

An exact analytic solution for  $J$  is generally nonexistent, and approximate, asymptotic

solutions such as those valid for large  $k$ , that is, a wavelength much smaller than any other length scale, become relevant. The usual asymptotic (subscript a) solution takes the form (2)

$$J_a(x'', R; x', 0) = \sum \{k/[2\pi i \tilde{x}(R)]\}^{1/2} e^{ikS(x''; x')} \quad (4)$$

Here

$$S(x''; x') \equiv$$

$$\int_0^R [p(z)\dot{x}(z) - H(p(z), x(z), z)] dz \quad (5)$$

where the functions  $p(z)$  and  $x(z)$  are solutions, based on the real Hamiltonian function  $H$ , of Hamilton's equations of motion,

$$dx(z)/dz \equiv \dot{x}(z) = \partial H / \partial p(z) \quad (6)$$

$$dp(z)/dz \equiv \dot{p}(z) = -\partial H / \partial x(z) \quad (7)$$

subject to the boundary conditions

$$x(R) = x'', \quad x(0) = x' \quad (8)$$

Equation 6 may be inverted to give  $p = p(\dot{x}, x, z)$ , which then defines  $p$  in terms of the slope  $\dot{x}$  and position  $(x, z)$ . We assume there is at least one such solution to Eqs. 6 and 7 consistent with Eq. 8, which is referred to as a ray: if there is more than one ray then the sum in Eq. 4 implicitly includes them all. The amplitude coefficient, which involves the factor  $[\tilde{x}(R)]^{-1/2}$ , reflects the local density of rays. Here  $\tilde{x}(z)$  and its partner  $\tilde{p}(z)$  denote solutions of the linearized equations of motion, about each relevant ray. These equations are

$$\dot{\tilde{x}}(z) = H_{px}(z)\tilde{x}(z) + H_{pp}(z)\tilde{p}(z) \quad (9)$$

$$\dot{\tilde{p}}(z) = -H_{xx}(z)\tilde{x}(z) - H_{xp}(z)\tilde{p}(z) \quad (10)$$

subject to the initial conditions  $\tilde{x}(0) = 0$  and  $\tilde{p}(0) = 1$ . Here, for example,  $H_{px}(z) \equiv \partial^2 H / \partial p \partial x$  evaluated along the principal ray solution of Eqs. 6 and 7. In other words, taken together Eqs. 6, 7, 9, and 10 relate to the trajectory of neighboring rays that begin at  $x'$  but with slightly different initial  $p$ -values than the principal ray.

The representation afforded by Eq. 4 is quite adequate unless  $\tilde{x}(R) = 0$  for some ray, which generally occurs at a caustic (defined as an envelope of ray crossings). Physically,  $\tilde{x}(R) = 0$  signifies that rays that start at  $x'$  and end at  $x''$  have a first-order insensitivity to the outgoing orientation about its nominal value. Consequently, we expect an enhancement of the field amplitude at such points, but the divergence offered by Eq. 4 is generally in error.

As a prelude to introducing an alternative to Eq. 4 we first observe that

$$J_a(x'', R; x', 0) = \sum \frac{k}{2\pi} \frac{1}{\sqrt{\tilde{p}(R)}} e^{ikS(x''; x')} \times \int_{-\infty}^{\infty} e^{-ik[\tilde{x}(R)/\tilde{p}(R)]u^2/2} du \quad (11)$$

holds as an identity. When armed with sufficient hindsight the combined phase factor in Eq. 11 may be recognized as a quadratic approximation within another integral representation given by (3)

$$J_a^M(x'', R; x', 0) \equiv \sum \frac{k}{2\pi} \frac{1}{\sqrt{\tilde{p}(R)}} \times \int_{-\infty}^{\infty} e^{ikp''x'' + ikS_M(p''; x')} dp'' \quad (12)$$

Here  $S_M$  is determined by a Legendre transformation of  $S$ , that is,

$$S_M(p''; x'') \equiv -p''x'' + S(x''; x') \quad (13)$$

with the right side evaluated at  $x'' = x''(p'', x')$  which comes from inverting  $p'' \equiv \partial S(x''; x') / \partial x''$ . A stationary-phase evaluation of Eq. 12 leads to

$$J_a^M(x'', R; x', 0) = \sum \frac{k}{2\pi} \frac{1}{\sqrt{\tilde{p}(R)}} e^{ikS(x''; x')} \times \int_{-\infty}^{\infty} e^{ikD_M(u)} du \quad (14)$$

where

$$D_M(u) \equiv (p'' + u)x'' + S_M(p'' + u; x') - S(x''; x') \quad (15)$$

with the right side evaluated at  $p'' = p''(x'', x')$  which in turn comes from inverting  $x'' \equiv -\partial S_M(p''; x') / \partial p''$ . As a stationary point and an inverse Legendre transformation it follows that  $D_M$  and  $\partial D_M / \partial u$

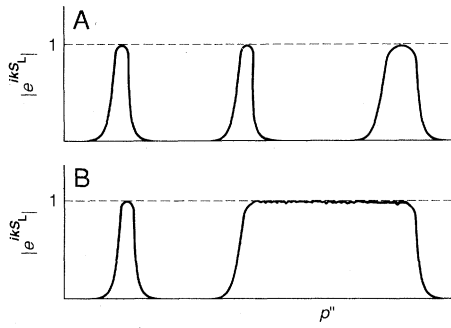


**Fig. 1.** (A) Schematic plot of  $|e^{ikS_L}|$  versus  $p''$  for a case with three rays. With  $x''$  and  $x'$  held fixed the three rays occur for those  $p''$  values where the curve reaches an amplitude of unity. Near each ray, where the curve is less than but near to unity, one is in a region that is strictly forbidden in the geometrical or zero-wavelength limit. For non-zero wavelengths such nearby regions contribute to the integral in Eq. 20 helping to determine the amplitude for the waveform associated with that particular ray. (B) Schematic plot of  $|e^{ikS_L}|$  versus  $p''$  for a case with one isolated ray and a finite band of a large number of closely spaced rays. For the isolated ray the discussion of (A) pertains. Within the band the curve reaches unit amplitude for each ray, and these are so closely spaced that for nonzero wavelength the curve remains very close to unity throughout the band. For the contribution to Eq. 17 it suffices to approximate the curve as being of unit amplitude within the interval of the band.

both vanish at  $u = 0$ . If  $D_M(u)$  may be approximated by a quadratic term, then Eq. 11 is recovered, and the amplitudes are proportional to  $k^{1/2}$ , as in Eq. 4. The merits of this approach arise at a caustic where the coefficient of the quadratic term in  $D_M(u)$  vanishes and the cubic term becomes relevant. When that is the case the partial amplitude in Eq. 14 is finite and proportional to the enhanced factor  $k^{2/3}$ . Moreover, if  $\tilde{x}(R) = 0$  then  $\tilde{p}(R) \neq 0$ , for if  $\tilde{x}$  and  $\tilde{p}$  vanish simultaneously then Eqs. 9 and 10 imply they vanish for all  $z$  including  $z = 0$  which is incompatible with the chosen initial condition. Although Eq. 14 is correct at caustics it generally fails at pseudocaustics, which are defined by the condition  $\tilde{p}(R) = 0$ . Since  $\tilde{x}(R) \neq 0$  at pseudocaustics one may skip back and forth between Eq. 4 and Eq. 14, using one when the other fails (3). However, when there are many caustics and pseudocaustics this ceases to be practical.

Yet another asymptotic approach may be introduced with the observation that

$$J_a(x'', R; x', 0) = \sum \frac{k}{2\pi} \times \frac{1}{\sqrt{\tilde{p}(R) + i\Omega\tilde{x}(R)}} e^{ikS(x'', x')} \times \int_{-\infty}^{\infty} e^{-ik\{\tilde{x}(R)/[\tilde{p}(R) + i\Omega\tilde{x}(R)]\}u^2/2} du \quad (16)$$

holds as an identity, where  $\Omega$  must be

positive for the integral to converge. The combined "phase factor" in this expression is generally not real, yet—and again when armed with sufficient hindsight—it may be recognized as a quadratic approximation within still another integral representation given by (4)

$$J_a^L(x'', R; x', 0) \equiv \frac{k}{2\pi} \int_{-\infty}^{\infty} \frac{1}{\sqrt{\tilde{p}(R) + i\Omega\tilde{x}(R)}} e^{ikS_L(p'', x'', x')} dp'' \quad (17)$$

where

$$S_L(p'', x'', x') \equiv [p'' + p(R)][x'' - x(R)]/2 + S(x(R); x') \quad (18)$$

As before  $p(z)$  and  $x(z)$  are solutions of Hamilton's equations, Eqs. 6 and 7, but now subject to the generally complex boundary conditions

$$p(R) + i\Omega x(R) = p'' + i\Omega x'', \quad x(0) = x' \quad (19)$$

To satisfy these boundary conditions set  $x(R) = x'' + w$  and  $p(R) = p'' - i\Omega w$  where  $w$  is a complex variable chosen so that  $x(0) = x'$ . If  $w = 0$ , then  $x(R) = x''$  and  $p(R) = p''$ , and it follows that  $S_L(p'', x'', x') = S(x'', x')$  for that particular (real) ray specified by  $p''$ . When  $w \neq 0$  it is noteworthy that  $\text{Im } S_L(p'', x'', x') > 0$ , or in other words  $|\exp(ikS_L)| < 1$ . Thus the dominant factor in the integrand of Eq. 17 is, for large  $k$ , extremely small except at and near those  $p''$  values that correspond to real rays between  $x''$  and  $x'$  (Fig. 1A). For sufficiently well-separated peaks, as depicted in Fig. 1A, an approximate evaluation of Eq. 17 is given by

$$J_a^L(x'', R; x', 0) = \sum \frac{k}{2\pi} \frac{1}{\sqrt{\tilde{p}(R) + i\Omega\tilde{x}(R)}} e^{ikS(x'', x')} \times \int_{-\infty}^{\infty} e^{ikD_L(u)} du \quad (20)$$

where

$$D_L(u) \equiv S_L(p'' + u, x'', x') - S(x'', x') \quad (21)$$

with the right side evaluated at  $p'' = p''(x'', x')$  corresponding to one of the real rays. It follows that  $D_L$  and  $\partial D_L/\partial u$  both vanish at  $u = 0$ . If  $D_L(u)$  may be approximated by a quadratic term, then Eq. 16 is recovered, and the amplitudes are proportional to  $k^{1/2}$ . At a caustic where the coefficient of the quadratic term in  $D_L(u)$  vanishes then the cubic term becomes relevant. As in the previous case the partial amplitude in Eq. 20 is finite and proportional to the enhanced value  $k^{2/3}$ . The slowly varying expression  $\tilde{p}(R) + i\Omega\tilde{x}(R)$  is evaluated at

each principal ray in Eq. 20, and based on earlier arguments, cannot vanish, implying that Eq. 20 is everywhere valid. Thus in Eq. 20 we have achieved a global, uniform asymptotic approximation valid when the rays are well separated in the sense that midway between the rays  $k \text{Im } S_L \gg 1$  (Fig. 1A).

It is interesting to observe that  $J_a^L$  interpolates between  $J_a$  and  $J_a^M$  in the sense that

$$\lim_{\Omega \rightarrow \infty} J_a^L(x'', R; x', 0) = J_a(x'', R; x', 0) \quad (22)$$

$$\lim_{\Omega \rightarrow 0} J_a^L(x'', R; x', 0) = J_a^M(x'', R; x', 0) \quad (23)$$

This interpolation is evident at the quadratic approximation level; for example, compare Eqs. 16 and 11 and as  $\Omega \rightarrow 0$ . But it also holds more generally, and it is from the limit  $\Omega \rightarrow \infty$  or  $\Omega \rightarrow 0$  that the finite amplitude coefficients of  $J_a^L$  in Eq. 20 develop singularities at caustics or pseudocaustics, respectively.

When there are many rays contributing, as is the generic situation for sufficiently large  $R$ , the conditions leading to Eq. 20 may not hold. In that case we deal directly with Eq. 17 (4). We may even suppose there is an interval  $\mathcal{R}$  of  $p''$  where the rays are so closely spaced (a "thicker") that for all  $p''$  in  $\mathcal{R}$ ,  $k \text{Im } S_L(p'', x'', x') \ll 1$  (Fig. 1B). Outside  $\mathcal{R}$  we illustrate in Fig. 1B a case of well-separated rays. The example of a vast number of rays illustrated in Fig. 1B may be dealt with as follows. Break up the integral in Eq. 17 into two disjoint pieces, one over  $\mathcal{R}$ , and the other over the complementary set  $\mathcal{R}'$ . Within  $\mathcal{R}'$  the procedure that led to Eq. 20 may be used. Within  $\mathcal{R}$  replace  $S_L$  by  $\text{Re } S_L$  in the exponent. Then evaluate both integrals by suitable stationary-phase approximations. As argued previously the amplitude factors in this formulation remain finite throughout. In this way Eq. 17 becomes a readily evaluated, global and uniform integral representation for fields having a vast number of contributing rays any number of which could be caustics.

Although our discussion of the three different asymptotic approximations has of necessity been somewhat of a caricature, the relative merits of these three approximations is faithfully represented. Extensions to transverse coordinates of more than one dimension and to multicomponent wave equations, which are available in the cited literature, do not materially affect the situation.

#### REFERENCES AND NOTES

1. See L. Brekhovskikh and Yu. Lupanov, *Fundamentals of Ocean Acoustics* (Springer, New York, 1982); A. K. Ghatak and K. Thyagarajan, *Contemporary Optics* (Plenum, New York, 1978), chap. 9.

2. See M. Born and E. Wolf, *Principles of Optics* (Pergamon, New York, ed. 3, 1965), chap. 3.
3. See V. P. Maslov and M. V. Fedoruk, *Semi-Classical Approximation in Quantum Mechanics* (Reidel, Dordrecht, 1981).
4. For the most complete account see, J. R. Klauder, *Ann. Phys. (N.Y.)* **180**, 108 (1987). For partial accounts see, J. R. Klauder, *Phys. Rev. Letters* **59**,

748 (1987); in *Random Media* (IMA Series in Mathematics and Its Applications), G. Papanicolaou, Ed. (Springer, New York, 1987), vol. 7, p. 163; and in *The Physics of Phase Space*, Y. S. Kim and W. W. Zachary, Eds. (Springer, Berlin, 1987), p. 290.

14 September 1987; accepted 14 December 1987

## Biologically Effective Ultraviolet Radiation: Surface Measurements in the United States, 1974 to 1985

JOSEPH SCOTTO, GERALD COTTON, FREDERICK URBACH,  
DANIEL BERGER, THOMAS FEARS

Recent reports of stratospheric ozone depletion have prompted concerns about the levels of solar ultraviolet radiation that reach the earth's surface. Since 1974 a network of ground-level monitoring stations in the United States has tracked measurements of biologically effective ultraviolet radiation (UVB, 290 to 330 nanometers). The fact that no increases of UVB have been detected at ground levels from 1974 to 1985 suggests that meteorological, climatic, and environmental factors in the troposphere may play a greater role in attenuating UVB radiation than was previously suspected.

RECENT REPORTS OF STRATOSPHERIC ozone depletion (1), as much as 40% over parts of Antarctica during its spring month of October (2), suggest that greater amounts of solar ultraviolet radiation will reach the surface of the earth. In 1974 a collaborative study of ground-level measurements of biologically effective, nonionizing solar radiation was implemented (3). We report trends in the annual amounts of biologically effective ultraviolet radiation (UVB, 290 to 330 nm) that reach the earth's surface at several locations within the United States. Solar ultraviolet radiation can produce skin erythema (sunburn) in humans and skin cancer in laboratory animals (4) and would be expected to increase if ozone is depleted. A 1% decrease in stratospheric ozone could cause about a 2% increase in the amount of UVB that would pass through this shield (5). The increases vary according to specific waveband, season, and zenith angle of the sun (6).

Photosensitive meters [Robertson-Berger (R-B) meters] were installed at various National Weather Service stations (usually airports) and have been monitored and maintained continuously since 1974 (Table 1). The locations span a latitude range from 30° to 47°N and a longitude range from 75.2° to 122.2°W. Radiation in the UVB range is monitored by a magnesium tungstate sensor and weighted according to an action spectrum that parallels that for skin erythema.

The most effective biological wavelength for producing erythema on typical Caucasian skin is 297 nm (7). The biological effectiveness of UVB decreases logarithmically within the UVB range; at 330 nm it is less than 0.1% as effective as at 297 nm. The R-B meter integrates the weighted amounts of UVB and provides counts in "sunburn units" (SU) (8-10). Quality control checks included an evaluation of diurnal, daily, and monthly readings at specific locations to verify that SU counts agreed with meteorological data.

To assure that the R-B meter measurements were comparable among stations, each meter was checked annually against two standardized meters, which were checked every other week against a calibrating light source (11). Calibration factors (CFs) (obtained for each year from 1974 to 1983 for each station) varied in absolute value among stations, but no significant annual trends in CF were noted for the stations reported here. Data presented for 1984 and 1985 were adjusted according to the most recent CF at each field station. The outputs from R-B meters have been compared with those from Dobson spectropho-

tometers (presently used for measuring total ozone) that were modified to provide measures of erythema UVB energy reaching the earth's surface at two stations, Bismarck, North Dakota, and Tallahassee, Florida (12). The correlation coefficients were reported to be 0.96 and 0.98, respectively, at these locations, and provided an estimate for the conversion of R-B meter readings to energy units (2.8 counts equal 1 J/m<sup>2</sup>).

Table 2 shows annual R-B measurements from the period from 1974 to 1985 at each station, arranged according to increasing latitude. The intensity of UVB at each station (Table 2) could have varied according to geographic factors, such as latitude, longitude, and altitude, and physical or meteorological factors, such as the water content of the atmosphere, turbidity, and cloudiness of the day. Solar UV flux generally decreases as latitude increases and as the zenith angle increases. However, Tallahassee, the southernmost station, received less solar UV than either Albuquerque, New Mexico, or El Paso, Texas. This difference reflects the effect of the higher altitude and less turbid and cloudy conditions at the southwestern stations compared to the Florida station, which has greater amounts of sky cover and humidity.

Average annual R-B counts for two consecutive 6-year periods (1974 to 1979 and 1980 to 1985) show a negative shift at each station, with decreases ranging from 2 to 7% (Table 2). Figure 1 (semi-logarithmic plot) shows that there are no positive trends in annual R-B counts for 1974 to 1985. The logarithm of the annual R-B counts is used as the dependent variable in regression analyses to obtain an estimate of the average annual percentage change. The estimated average annual change varied from -1.1% at Minneapolis, Minnesota, to -0.4% at Philadelphia, Pennsylvania (Table 2). For all the stations the R-B counts dropped an average of 0.7% per year since 1974. Three of the individual station trend coefficients were not statistically significant, however.

Although we rule out changes in instrumentation and monitoring techniques, it is unclear whether abrupt meteorological changes such as atmospheric aerosol scatter-

**Table 1.** Geographic locations and meteorological measures for the eight stations used.

Site number	Location	Latitude (°N)	Longitude (°W)	Elevation (m)	Average sky cover
1	Tallahassee, FL	30.4	84.4	2	0.58
2	El Paso, TX	31.8	106.4	1194	0.39
3	Fort Worth, TX	32.8	97.0	164	0.52
4	Albuquerque, NM	35.0	106.6	1619	0.44
5	Oakland, CA	37.7	122.2	2	0.48
6	Philadelphia, PA	39.9	75.2	9	0.62
7	Minneapolis, MN	44.9	93.2	255	0.64
8	Bismarck, ND	46.8	100.7	502	0.63

J. Scotto and T. Fears, Biostatistics Branch, National Cancer Institute, Bethesda, MD 20892.

G. Cotton, Air Resources Laboratory, National Oceanic and Atmospheric Administration, Silver Spring, MD 20910.

F. Urbach and D. Berger, Health Sciences Center, Temple University, Philadelphia, PA 19140.